Neutron capture cross sections of ^{112,116,122,124}Sn

K. S. Krane and J. Sylvester
Department of Physics, Oregon State University, Corvallis, Oregon 97331, USA
(Received 3 January 2006; published 19 May 2006)

The thermal cross sections and resonance integrals have been determined for radiative neutron capture by ^{112,116,122,124}Sn leading to the ground and isomeric states of ^{113,123,125}Sn and the isomeric state of ^{117}Sn. Using natural samples of Sn metal foils and high-resolution γ-ray spectroscopy, it was possible to determine a mutually consistent set of cross sections, particularly the small thermal cross sections leading to $11/2^-$ states. A detailed analysis of the γ-ray emissions from irradiated Sn samples enabled us to make new and more precise determinations of the energies and intensities of γ rays emitted in the decays of 40-min ^{123m}Sn and 9.5-min ^{125m}Sn and corresponding adjustments to the energy levels of ^{123,125}Sb. The present results support the recently adopted revised value for the branching ratio of the 255.1-keV γ ray in the decay of ^{113}Sn. The presence of a ^{116m}In impurity in our samples prompted a new determination of the energies and intensities of the γ rays emitted in its decay and of the energy levels in ^{116}Sn.

DOI: 10.1103/PhysRevC.73.054312 PACS number(s): 21.10.−k, 25.40.Lw, 27.60.+j, 23.20.Lv

I. INTRODUCTION

Precise and consistent values of neutron capture cross sections are important not only for the characterization of materials using neutron activation analysis but also as a probe of nuclear systematics. Thermal cross sections provide a convenient fixed calibration point for calculations that seek to characterize neutron interactions in other energy regions, such as at stellar temperatures.

The cross sections for neutron capture by Sn isotopes have been previously measured in a variety of studies using the activation technique of measuring the radiations emitted in radioactive decays that follow neutron capture [1,2]. In some previously reported cases, it was not possible to distinguish clearly between captures leading to ground and isomeric states, and many previous studies used detectors of poor resolution in comparison with present capabilities. Consequently, there is a wide variation and often poor agreement among the results reported from previous studies.

In the present work, we sought to remeasure these thermal cross sections and resonance integrals in a consistent manner to provide a set of results that enables the reliable comparison of ground-state and isomeric cross sections as well as comparison of results for different Sn isotopes. We were particularly concerned with obtaining values for the millibarn cross sections for thermal captures leading to the $11/2^-$ states in ^{117,123,125}Sn, as these values have appeared in previous studies with large relative uncertainties (including one study yielding a negative cross section). The extraction of such small thermal cross sections generally involves a careful correction for the effects of capture of epithermal neutrons, and so we also sought to obtain a precise and consistent set of resonance integrals.

A schematic view of the neutron capture process applicable to the even-mass Sn isotopes is shown in Fig. 1. Capture by an even-mass Sn isotope of mass number A leads eventually to the ground state and an isomeric state in the Sn isotope of mass number $A+1$. Isotopic and decay parameters relevant to the present investigation are listed in Table I [3]. For ^{113m}Sn and ^{117m}Sn, the isomeric state decays mostly or entirely through an isomeric $\gamma+e$ transition, which serves as the analyzer for that state. For ^{123m}Sn and ^{125m}Sn, there is no isomeric transition, so the decays of both the isomeric and ground states are analyzed through γ transitions in the Sb isotopes populated following the Sn β decay.

The energies and intensities of the γ rays in ^{123,125}Sb following the decays of ^{123m,125m}Sn are known only with relatively large uncertainties. We have therefore studied the decays of irradiated Sn samples with a high-resolution spectroscopy system in order to improve the spectroscopic knowledge of these decays. We report here the results of these studies, along with the verification of a newly proposed branching ratio in the decay of ^{113}Sn and a spectroscopic study of the decay of ^{116m}In, which is present as an impurity in our irradiated Sn samples.

II. EXPERIMENTAL DETAILS

Samples of Sn metal foils of thickness 0.025 mm were irradiated in the Oregon State TRIGA reactor (OSTR) [4]. Four different irradiation facilities were used: a thermal column (TC; nominal thermal and epithermal neutron fluxes of, respectively, 7.2×10^{10} and 1.8×10^{8} neutrons/cm^2-s), in-core irradiation tube (ICIT; 9×10^{12} and 1×10^{12} neutrons/cm^2-s), a cadmium-lined in-core irradiation tube (CLICIT; 0 and 1×10^{12} neutrons/cm^2-s), and a fast pneumatic transfer facility ("rabbit"; 1×10^{13} and 4×10^{11} neutrons/cm^2-s). The rabbit samples could also be enclosed in a Cd box (1-mm wall thickness) to isolate the epithermal component. All Sn irradiations were accompanied by flux monitors. Primary flux monitors were Au and Co as dilute alloys (respectively, 0.134% and 0.438%) in thin Al metal foils. Secondary flux monitors were Fe, Zn, and Zr, also as thin metal foils. Properties of these flux monitors have been discussed previously [5].

The Sn samples for irradiation ranged from about 20 to 600 mg. The larger samples were placed into storage for several months to allow the 9.64-d ^{125}Sn to decay, which enabled the weak 1089-keV line in the decay of ^{123}Sn to be clearly seen without interference from the ^{125}Sn line of the

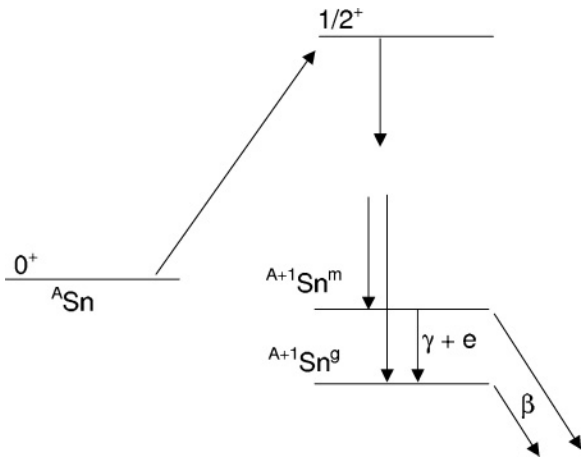

FIG. 1. Processes involved in thermal neutron capture by even-mass Sn isotopes. In the capture of epithermal neutrons, p-wave ($3/2^-$) resonances may also contribute.

same energy. Irradiations in the TC, ICIT, and CLICIT were of typical durations of 1 to several hours. Counting of some of the TC samples began as soon as 45 min after the irradiation, permitting observation of the short-lived ^{113m,123m,125m}Sn. Rabbit irradiations to observe these same short-lived activities were typically 5 min long, and counting began within 15 min after irradiation.

The γ rays were observed with a high-purity Ge detector (nominal volume of 169 cm^3, efficiency of 35% compared with NaI at 1332 keV, resolution of 1.68 keV at 1332 keV). Source-to-detector distances were generally 10 to 20 cm, for which coincidence summing has a negligible effect on the intensities of the strongest transitions; the weak ^{123}Sn samples, which are not affected by coincidence summing, were counted at 7.5 cm. The signals were analyzed with a digital spectroscopy system connected to a desktop computer. For the cross-section determinations, peak areas of the γ-ray lines, which were well isolated from neighboring peaks, were usually determined with the MAESTRO software [6]. The spectroscopy studies were analyzed using the spectrum analysis software SAMPO [7]. Absolute efficiency calibrations were done with NIST-traceable sources of ^{133}Ba and ^{152}Eu. The relative efficiency calibration below 200 keV was characterized using reactor-produced sources of ^{160}Tb, ^{169}Yb, and ^{182}Ta; above 1500 keV, ^{24}Na and ^{207}Bi were used. Sample γ-ray spectra from the long- and short-lived Sn activities are shown in Figs. 2 and 3. To be able to account properly for the effect of the intense ^{116m}In activity in the short-lived sample, a separate measurement was made of the ^{116m}In γ rays from a small sample of irradiated In.

III. CROSS-SECTION RESULTS

After correcting for detector efficiency and source decay, the deduced activities at the end of bombardment were typically in the range of 10–100 kBq for the long-lived isotopes produced in the ICIT and CLICIT irradiations, 100 Bq and 100 kBq for, respectively, the long- and short-lived isotopes in the TC irradiations, and 1–10 MBq for the short-lived isotopes produced in the rabbit irradiations. Also present in our samples were ^{125}Sb (produced from the decay of ^{125}Sn) and activities of ^{110m}Ag, ^{116m}In, and ^{122,124}Sb, presumably produced from neutron capture by small Ag, In, and Sb impurities present in the Sn. None of these activities interfered with the measurement. Because the ^{125}Sb observed in the ICIT and CLICIT samples is produced almost entirely from the decay of ^{125m}Sn, the ^{125}Sb provided an independent check on the cross sections deduced from the ^{125m}Sn in the TC and rabbit irradiations.

The end-of-bombardment Sn activity a resulting from irradiation of N target nuclei for a time t_i can be represented as

$$a = N(\phi_{\rm th}\sigma + \phi_{\rm epi} I)(1 - e^{-\lambda t_i}), \qquad (1)$$

where $\phi_{\rm th}$ and $\phi_{\rm epi}$ and the thermal and epithermal neutron fluxes and σ and I represent the effective thermal cross section and resonance integral. According to the resonance data presented in Ref. [1], there are no broad or low-energy neutron resonances in any of the isotopes considered in the present work; therefore, the cross section below 1 eV follows the expected $1/v$ behavior. The flux monitors behave similarly, so our data give the equivalent 2200 m/s thermal cross section. Because the thermal cross sections of all the final states considered in this work are much smaller than the resonance integrals, the correction for the $1/v$ contribution to

TABLE I. Properties of Sn isotopes used for cross-section determinations.

A	Abundance (%)	Capture to	J^π	$t_{1/2}$	Isomeric state		Analyzing γ transitions
					E (keV)	$I_{\gamma+e}$ (%)	
112	0.97	113 g	$1/2^+$	115.09 d			255.1 (2.1%), 391.7 (65.0%)
		113 m	$7/2^+$	21.4 min	77.4	91.1	77.4 (0.50%)
116	14.54	117 g	$1/2^+$	∞			
		117 m	$11/2^-$	13.61 d	314.6	100	156.0 (2.1%), 158.6 (86.4%)
122	4.63	123 g	$11/2^-$	129.2 d			1088.6 (0.60%)
		123 m	$3/2^+$	40.08 min	24.6	0	160.3 (85.6%)
124	5.79	125 g	$11/2^-$	9.64 d			822.4 (4.0%), 915.5 (3.9%), 1067.0 (9.0%), 1087.6 + 1089.2 (5.4%)
		125 m	$3/2^+$	9.52 min	27.5	0	332.0 (97.0%)

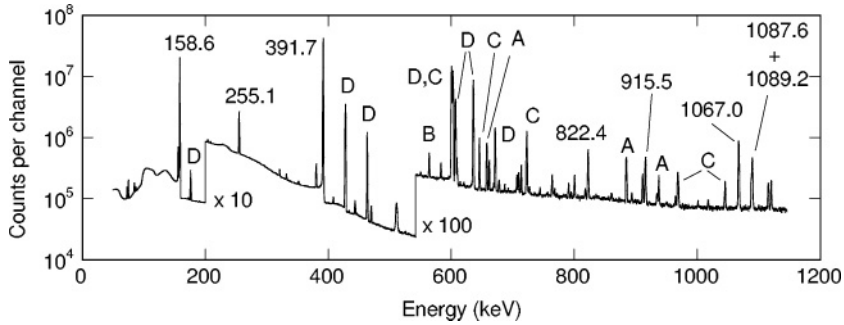

FIG. 2. γ-ray spectrum of long-lived activities from irradiated Sn. Peaks from Sn decays used in cross-section determination are labeled with their energies in keV. Prominent impurity peaks include those from ^{110m}Ag (A), ^{122}Sb (B), ^{124}Sb (C), and ^{125}Sb (D).

the resonance integral is negligible, except for captures leading to ^{123m}Sn, where it contributes at about the level of one standard deviation of I.

The thermal cross sections deduced in the present work are shown in Table II and compared with results of previous studies [8–21]. The uncertainties are typically in the 5%–10% range and represent mostly uncertainties in the flux measurements and detector efficiency calibrations; uncertainties due to counting statistics were generally negligible, as were contributions to the overall uncertainty from the γ-ray branching ratios (except as discussed below). The relatively large uncertainty in the thermal cross section for ^{123g}Sn is due to the uncertainty in the correction for epithermal captures in the ICIT irradiations. (The otherwise similar results for ^{125g}Sn do not show this effect because the latter were obtained from the TC irradiations for which the epithermal correction is much smaller; unfortunately, the ^{123g}Sn was too weak to be seen in the TC samples.) For ^{123g}Sn and ^{125g}Sn, we have *not* included in the uncertainty a possible systematic effect in the absolute branching intensities, estimated to be, respectively, 17% and 29% [3].

Although it is not always clear from the previous works, the results quoted for the cross section leading to ^{113g}Sn represent a combination of direct and indirect production through the decay of the isomer. Using the present results for the cross sections leading to the isomer, we can obtain the cross section for direct production of ^{113g}Sn by neutron capture, which is indicated in Table II.

The ratio between the isomeric and ground-state thermal cross section was measured for ^{113}Sn by Schmorak *et al.* [10] and for ^{113}Sn and ^{123}Sn by Gangrsky *et al.* [22]. For ^{113}Sn, our results give $\sigma(\mathrm{m})/\sigma(\mathrm{g}) = 0.36 \pm 0.08$, in excellent agreement with the previous results (0.41 ± 0.06 [10] and 0.41 ± 0.03 [22]). For ^{123}Sn, the present results give a ratio of 34 ± 10, which does not agree very well with the previous results (14.3 ± 1.6, [22]).

TABLE II. Thermal cross sections of Sn isotopes.

Product	σ (b)	
	Present work	Previous work
113 g+m	0.513 (30)	1.1 (4)[a], 1.3 (3)[b], 0.9 (3)[c], 0.65[d], 0.71 (10)[e], 0.52[f], 0.42 (8)[g], 0.576 (12)[h], 0.547 (30)[i], 0.539 (11)[j]
113 g	0.386 (38)	
113 m	0.140 (26)	0.39 (10)[c]
117 m	0.0035 (5)	0.006[b], −0.015 (1)[h], 0.00542 (30)[i]
123 g	0.0041 (12)	0.1[b]
123 m	0.138 (10)	0.1[b], 0.206 (30)[k], 0.15 (2)[e], 0.145[f], 0.18 (2)[g], 0.134 (15)[h], 0.19 (6)[l]
125 g	0.0033 (3)	0.002[b], 0.0042 (13)[m]
125 m	0.114 (10)	0.57 (11)[a], 0.5[b], 0.125 (19)[k], 0.13 (2)[e], 0.11 (4)[g], 0.135 (5)[n], 0.070 (4)[h], 0.43 (6)[l]

[a]Reference [8].
[b]Reference [9].
[c]Reference [10].
[d]Reference [12].
[e]Reference [13].
[f]Reference [14].
[g]Reference [15].
[h]Reference [17].
[i]Reference [18].
[j]Reference [19].
[k]Reference [11].
[l]Reference [20].
[m]Reference [21].
[n]Reference [16].

TABLE III. Resonance integrals of Sn isotopes.

Product	I (b)	
	Present work	Previous work
113 g+m	25.9 (21)	24[a], 25.4[b], 21 (4)[c], 28.7 (15)[d], 27.9 (16)[e], 189 (86)[f], 31 (6)[g]
113 g	20.0 (16)	
113 m	7.4 (6)	
117 m	1.43 (12)	1.86 (5)[d], 1.014 (20)[a]
123 g	0.100 (8)	1.06 (45)[f]
123 m	0.74 (5)	0.79[b], 0.71 (7)[c], 1.28 (20)[d]
125 g	0.103 (8)	0.083 (25)[h]
125 m	7.2 (5)	6.9 (10)[c], 7.5 (1)[i], 7.52 (35)[d], 16.7 (137)[f]

[a]Reference [12].
[b]Reference [14].
[c]Reference [15].
[d]Reference [17].
[e]Reference [18].
[f]Reference [23].
[g]Reference [24].
[h]Reference [21].
[i]Reference [16].

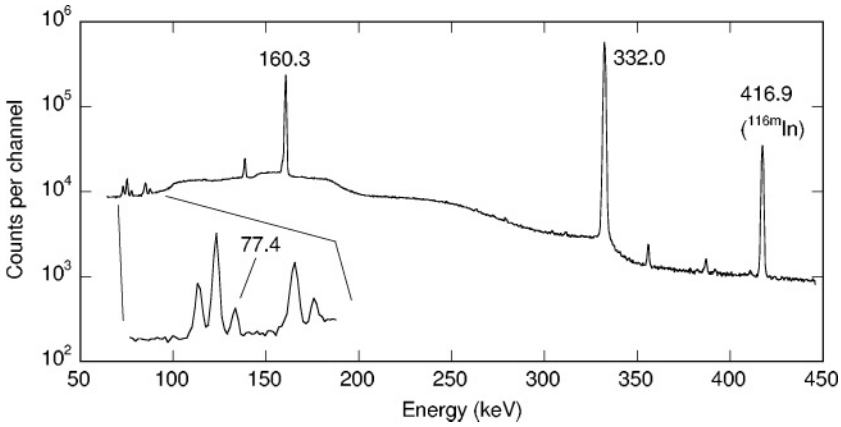

FIG. 3. γ-ray spectrum of short-lived activities from irradiated Sn, showing peaks used for cross-section determinations and a strong peak from the ^{116m}In impurity. The inset shows the 77.4-keV line in the region of the Pb x rays.

Resonance integrals measured in the present study are summarized in Table III and compared with results of previous work [23,24]. As was the case with the thermal cross sections, there is overall good agreement between the present and previous work. Several authors [25–27] have reported experimental values for the ratio I/σ. Their values are compared with those of the present work in Table IV. (The authors of Ref. [25] did not quote uncertainties for their values of I/σ. We assumed their quoted uncertainties for their deduced values of I from the ratio were characteristic of their errors in I/σ, since they apparently did not take into account the uncertainties in the previous values of σ from the literature.) The agreement is adequate except for the case of ^{117m}Sn, in which the extremely small value of the thermal cross section may be distorting the previous results; we found that even in our well-thermalized neutron beam there are still sufficient epithermals to require a correction to the deduced cross section. It is also possible that the results for ^{117m}Sn can be distorted by the ^{116}Sn(n, n') reaction; however, if this reaction were contributing to the present work our deduced value for I/σ would be even larger than the value quoted in Table IV.

IV. γ-RAY SPECTROSCOPY OF ^{113,123,125}Sn AND ^{116m}In

A. Decay of ^{113}Sn

In analyzing our data for the decay of ^{113}Sn, we used the value of 0.0325 for the ratio of the intensities of the 255.1- and 391.7-keV lines, taken from the online compilation of the NNDC [2]. This value disagrees with the previous value of 0.0285 quoted in the *Table of Radioactive Isotopes* [3] and the *Nuclear Data Sheets* [28]. We remeasured this ratio and obtained the value 0.0323 ± 0.0005, in agreement with the value adopted by the NNDC and with the most recent experimental determination (0.0337 ± 0.0005) by Mukherjee *et al* [29]. Our measurement includes data from five different samples of strengths varying by more than an order of magnitude and at counting distances from 10 to 20 cm; these measurements yield identical values for the branching ratio (within $\pm$ 0.5%).

B. Decay of ^{123m}Sn

Samples containing the short-lived Sn activities were produced by irradiating Sn in the rabbit for several minutes. Counting generally began within 5 min after irradiation. The ^{123m}Sn activity at the start of counting was typically in the range 0.2–1.0 MBq. Counting began with the sample at 20 cm from the Ge detector; after 30-50 min, the sample was moved to 10 cm. Even at the closer distance, coincidence summing produced negligible effects. A sample γ-ray spectrum is shown in Fig. 4.

The results of our measurements of the energies and intensities of the γ rays from the decay of ^{123m}Sn are shown in Table V and compared with the presently accepted values from the *Nuclear Data Sheets* [30], which are based on the weighted average of the results obtained by Raman *et al*. [31] and Tikku *et al*. [32]. Our data represent an average of the results from five different samples. We adjusted the ^{123}Sb level energies to fit our results for the γ-ray energies; the correspondingly deduced level energies are shown in Table V and listed with

TABLE IV. Ratio of resonance integrals to thermal cross sections.

Capture to	I/σ	
	Present work	Previous work
113 g+m	50.5 (50)	38.6 (19)[a], 49.1 (14)[b]
117 m	409 (49)	81 (3)[a], 60 (3)[c]
123 m	5.36 (53)	5.55 (13)[a], 5.37 (3)[b]
125 m	63 (7)	62 (3)[a], 53.0 (23)[b]

[a]Reference [25].
[b]Reference [27].
[c]Reference [26].

TABLE V. γ rays from the decay of ^{123m}Sn.

Present work				*Nuclear Data Sheets*[a]	
E (keV)	I	E_i	E_f	E (keV)	I
160.35 *3*	100 *2*	160.35	0.0	160.32 *5*	100
171.22 *38*	0.003 *3*	712.79	542.06	170.9 *7*	0.008 *5*
381.77 *5*	0.050 *3*	542.06	160.35	381.4 *3*	0.049 *4*
541.95 *10*	0.028 5	542.06	0.0	541.8 *4*	0.023 *4*
552.29 24	0.010 *3*	712.79	160.35	552.5 *3*	0.012 *2*

[a]From Ref. [30], based on data of Raman *et al*. [31] and Tikku *et al*. [32].

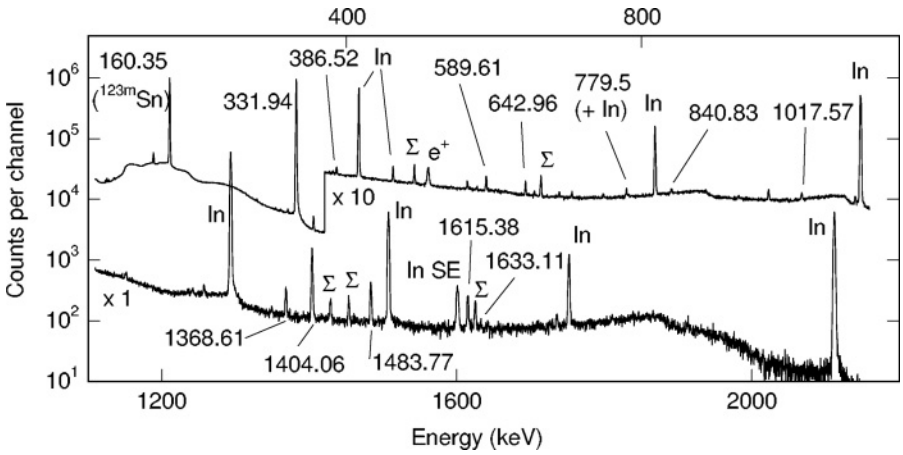

FIG. 4. γ-ray spectra from the decay of ^{123m}Sn and ^{125m}Sn. Peaks from these decays are labeled with their energies in keV. Peaks from ^{116m}In (In), coincidence summing (Σ), and positron annihilation (e^+) are also labeled.

their uncertainties in Table VI. From our γ-ray intensities and the known [30] internal conversion coefficients, we deduced the β feeding intensities shown in Table VI. Overall, the present results are in agreement with and are more precise than the previously accepted values.

C. Decay of ^{125m}Sn

The ^{125m}Sn activity in the rabbit samples at the start of counting was typically about 2 MBq. Some of the stronger peaks in the γ-ray spectrum are labeled in Fig. 4. Table VII shows our deduced γ-ray energies and intensities compared with the previously accepted values from the *Nuclear Data Sheets* [33], which were obtained from an unweighted average of the data from Baedecker and Walters [34], Berzins and Auble [35], and Kawase *et al*. [36]. The uncertainties of our energies and intensities are generally an order of magnitude smaller than those of the previously accepted values. The decay with time was verified with the expected 9.5-min half-life for all peaks with intensity greater than 0.030; several peaks below that intensity also show agreement with the expected half-life (1304.42, 1349.37, 1633.11, and 1913.66 keV). The remaining peaks are either too weak to permit a half-life determination or contain admixtures of transitions from the decay of ^{116m}In.

In only three instances did we observe interference between the γ rays from ^{125m}Sn and those from the ^{116m}In impurity. The 278.56- and 779.5-keV γ rays are almost degenerate with ^{116m}In γ rays. By carefully measuring the intensities of the ^{116m}In components in a separate measurement with a pure ^{116m}In sample, it was possible to correct for the ^{116m}In components and thus obtain the intensities of the ^{125m}Sn components. Averaged over the course of the ^{125m}Sn counting, the combined 278-keV peak consisted of roughly 50%^{125m}Sn and 50%^{116m}In, while the 779-keV peak was about 25%^{125m}Sn and 75%^{116m}In. It was not possible to observe or resolve any doublet structure in the peaks at either energy; as a result, the deduced uncertainties of the ^{125m}Sn peak energies are larger than those of well-resolved peaks. The third peak that showed interference from ^{116m}In was at 2113 keV. Here, previous work shows a very weak ^{125m}Sn peak, which we could not observe because it was totally obscured by a very strong ^{116m}In peak at that energy.

We observed two peaks that have not been reported previously, at 430.03 and 1025.46 keV. We placed those peaks in the ^{125}Sb level scheme based on their good match with energy differences among known levels. We also observed a peak at an energy of 1633.11 keV, which was previously reported but does not fit among any of the known ^{125}Sb levels, even though its decay with time appears to be consistent with the expected 9.5-min half-life.

Based on our measured γ-ray energies and intensities, we deduced the level energies and β feedings shown in Table VIII. These are in good agreement with, but more precise than, the previously accepted values.

TABLE VI. Energy levels in ^{123}Sb populated in the decay of ^{123m}Sn.

Present work		*Nuclear Data Sheets*[a]		
Level energy (keV)	β feeding (%)	Level energy (keV)	β feeding (%)	J^π
0.00		0.00		$7/2^+$
160.35 *3*	99.92 *1*	160.33 *5*	99.92 *24*	$5/2^+$
542.06 *5*	0.065 *5*	541.8 *3*	0.055 *7*	$3/2^+$
712.79 *21*	0.011 *4*	712.8 *3*	0.017 *5*	$1/2^+$

[a]From Ref. [30].

D. Decay of ^{116m}In

Because it was necessary to make a precise correction for the presence of the 54-m ^{116m}In impurity in the Sn samples, we irradiated a small sample (roughly 0.1 mg) of In metal for 5 s in the rabbit facility, which produced a sample of ^{116m}In with an activity of 1.5 MBq. This sample was counted for 2 h at 20 cm and then for 2 h at 10 cm. To obtain precise energies for the stronger peaks, the sample was then returned to 20 cm and counted simultaneously with energy calibration sources (^{198}Au, ^{207}Bi, ^{60}Co, ^{137}Cs). Removal of some of the Pb shielding around the Ge detector allowed the background lines at 1460.83 and 2614.53 keV to be used for calibration, and Pb x rays from the remaining shielding provided low-energy calibration points. This process enabled a precise determination to be made of the energies of the eight ^{116m}In γ rays with intensities above 1%. These could then be used in turn to calibrate the high-count-rate spectra for the

TABLE VII. γ rays emitted in the decay of ^{125m}Sn.

Present work				*Nuclear Data Sheets*[a]	
E (keV)	I	E_i	E_f	E (keV)	I
278.56 *15*	0.023 *6*	921.55	642.96	278.4 *5*	0.07 *5*
310.96 *4*	0.045 *5*	642.96	331.94	311.2 *5*	0.07 *5*
331.94 *2*	100 *1*	331.94	0.0	331.9 *2*	100 *2*
386.52 *3*	0.100 *3*	1736.00	1349.46	386.0 *4*	0.09 *1*
430.03 *14*	0.012 *3*	1913.66	1483.77		
589.61 *2*	0.194 *4*	921.55	331.94	589.6 *5*	0.21 *4*
642.96 *2*	0.156 *3*	642.96	0.0	643.0 *5*	0.16 *4*
779.5 *3*	0.014 *4*	1700.55	921.55	778 *2*	0.013 *5*
840.83 *5*	0.072 *3*	1483.77	642.96	840.9 *5*	0.07 *2*
1017.57 *4*	0.087 *3*	1349.46	331.94	1017.3 *5*	0.10 *2*
1025.46 *22*	0.013 *6*	1947.32	921.55		
1057.77 *21*	0.019 *4*	1700.55	642.96	1059 *1*	0.02 *2*
1093.27 *14*	0.036 *3*	1736.00	642.96	1093 *1*	0.04 *2*
1151.70 *8*	0.032 *3*	1483.77	331.94	1151.1 *6*	0.03 *2*
1304.42 *10*	0.012 *3*	1947.32	642.96	1305 *1*	0.01 *1*
1349.37 *8*	0.017 *2*	1349.46	0.0	1349.0 *8*	0.02 *1*
1368.61 *4*	0.104 *3*	1700.55	331.94	1368.8 *5*	0.10 *2*
1404.06 *2*	0.699 *7*	1736.00	331.94	1404.0 *5*	0.72 *3*
1483.77 *2*	0.178 *3*	1483.77	0.0	1483.9 *5*	0.19 *3*
1581.96 *20*	0.010 *2*	1913.66	331.94	1582 *1*	0.006 *6*
1615.38 *3*	0.111 *3*	1947.32	331.94	1615.3 *5*	0.12 *2*
1633.11 *10*	0.016 *1*			1634 *1*	0.02 *2*
1736.07 *7*	0.031 *2*	1736.00	0.0	1735.6 *5*	0.03 *1*
1913.66 *10*	0.019 *2*	1913.66	0.0	1913.5 *5*	0.02 *1*
1947.50 *13*	0.014 *3*	1947.32	0.0	1947 *1*	0.010 *5*
–[b]				2113 *1*	0.002 *2*

[a]From Ref. [33], based on data from Baedecker and Walters [34], Berzins and Auble [35], and Kawase *et al*. [36].
[b]Not observable in present work due to interference from ^{116m}In.

determination of the energies of the weak peaks. A sample γ-ray spectrum is shown in Fig. 5.

At the high count rates used in this experiment, coincidence summing has a significant effect on the spectrum. The reduction in intensity of the strong peaks due to the "summing out" correction is small, but the "summing in" correction can distort the intensity of weak peaks and give rise to spurious peaks. Both true and accidental coincidences can contribute to the sum peaks. At the 20 cm distance, the average true/accidental ratio was about 0.6; and at 10 cm, the average ratio was about 3. It is also necessary to take into account the angular correlation effect in the true coincidences, which can increase the true coincidences by 10%–20% in some cases.

Our results for the energies and intensities of the γ rays following the ^{116m}In decay are shown in Table IX and compared with the previously accepted values from the *Nuclear Data Sheets* [37], based on a weighted average of the data reported by Rabenstein [38] and Ardisson [39]. Agreement with the expected 54-m half-life was checked for all transitions with intensities above 0.030 and for several below that level. Using our values for the γ-ray energies, we adjusted the energies of the ^{116}Sn levels to obtain the best

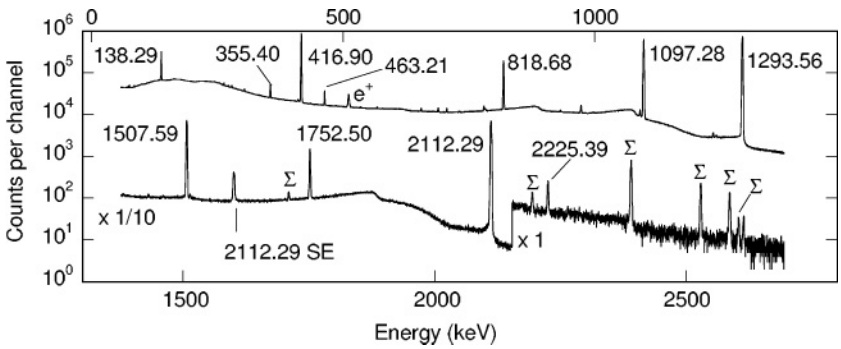

FIG. 5. γ-ray spectrum from the decay of ^{116m}In. Peaks are labeled with their energies in keV. Also labeled are peaks due to coincidence summing (Σ) and positron annihilation (e^+).

TABLE VIII. Energy levels in ^{125}Sb populated in the decay of ^{125m}Sn.

Present work		*Nuclear Data Sheets*[a]		
Level energy (keV)	β feeding (%)	Level energy (keV)	β feeding (%)	J^π
0.00		0.00		$7/2^+$
331.94 *2*	98.34 *2*	332.14 *4*	98.3 *20*	$5/2^+$
642.96 *2*	0.038 *11*	643.2 *3*	<0.11	$3/2^+$,$5/2^+$
921.55 *3*	0.185 *8*	921.7 *4*	0.26 *7*	$1/2^+$
1349.46 *5*	0.004 *4*	1349.46 *4*	0.029 *24*	$(7/2)^+$
1483.77 *2*	0.268 *5*	1484.1 *6*	0.28 *4*	$3/2^+$,$5/2^+$
1700.55 *4*	0.133 *6*	1700.9 *5*	0.13 *3*	
1736.00 *3*	0.842 *9*	1735.7 *3*	0.86 *4*	$(3/2)^+$
1913.66 *10*	0.040 *3*	1913.5 *5*	0.025 *12*	
1947.32 *3*	0.146 *5*	1947.4 *5*	0.136 *23*	$(3/2)^+$
		2113 *1*	0.002 *2*	$1/2^-$,$3/2^-$

[a]From Ref. [33].

agreement. The corresponding level energies are included in Table IX. The energies and their uncertainties are summarized in Table X along with the deduced β feedings (using the internal conversion coefficients given in Ref. [37]).

In general, our results are in good agreement with the previously accepted values. Among the differences are several peaks that we observe that have not been reported in previous works. A peak at 410.20 keV fits nicely between the 2801.17 and 2390.86 keV levels ($\Delta E = 410.31$ keV) and decays at a rate consistent with the 54-m half-life expected for ^{116m}In. A peak at 517.6 ± 0.9 keV was previously reported by Rabenstein [38] but has not yet been included in the accepted ^{116}Sn level scheme. We observe a γ ray at 517.23 ± 0.10 keV that can be placed between the levels at 3046.05 and 2529.13 keV ($\Delta E = 516.92$ keV). We observe a peak at 2265.69 keV that may be the ground-state transition from a previously known level at that energy. A γ ray at 1356.36 keV may be the transition from the previously known level at 2650.44 keV to the first excited state, and a γ ray at 395.64 keV could populate that level from the level at 3046.05 keV. We also observe a new transition at 1803.43 keV that can be placed between previously known levels at 3096.80 and 1293.56 keV.

We deduce a 10% greater intensity for the 138.29-keV γ ray than the previously accepted results. Although our relative intensity differs from the latest NDS compilation, it agrees with the value 4.308 ± 0.032 reported recently by Wurdiyanto *et al*. [40] based on both singles and coincidence measurements. We observe a peak at 165.72 keV that appears to decay with the expected half-life (albeit with large uncertainty) and which fits between two established levels (2390.86 and 2225.39 keV). The only previous reference to a transition at this energy comes from the Coulomb excitation work reported by Kantele *et al*. [41], who deduce $B(E2) < 2$ Weisskopf units, which corresponds to an intensity of <0.00046 units on the scale of Table IX. We therefore regard our identification of this transition in the decay scheme as very tentative.

We do not observe several γ rays that were reported in previous works (116.5, 196.5, 345.2, 458.5, 474.9, 500.1, 639.1, 1254.1, 1536.3 keV) and can set upper limits on their intensities that are significantly below the previously reported intensities. We do observe a previously reported peak at 730.47 keV but we can account for all of its intensity as a double escape (DE) peak from the 1752.50 keV γ ray. The closest match among the ^{116}Sn levels (and the previously suggested placement of this transition connecting the 3096.80- and 2365.94-keV levels) would correspond to an energy difference of 730.86 keV, amounting to 6.5 standard deviations from the measured γ-ray energy and making it unlikely that this assignment is correct. The previously identified transition at 781.1 keV is a single-escape (SE) peak from the 1293.56-keV transition; its large width in our spectrum marks it either as an unresolved doublet or a SE peak. The intensity of the peak at 272 keV consists about 48% of a γ ray of energy 271.96 keV and 52% of the DE peak from the 1293.56 keV transition; without correcting for the DE peak, the observed energy of this line (271.75 ± 0.02 keV) would deviate considerably from the energy difference corresponding to its placement in the level scheme (272.04 keV).

We observe a peak at 1235.49 ± 0.03 keV, in apparent agreement with previous work. However, our calculations indicate that essentially all of the intensity of this peak can be accounted for by coincidence summing, about 65% from the $416.90 + 818.68$ keV sum and about 35% from the $138.29 + 1097.28$ keV sum. Accidental coincidences account for 27% of the intensity at 20 cm and 7% at 10 cm. Together, these contributions account for about 95% of the observed peak, leaving possibly 5% to represent a transition between the 2529.13- and 1293.56-keV levels. Absent this correction, the deduced relative intensity of the 1235.49-keV peak would increase by about a factor of 2.5 between the 20 cm and 10 cm data. Although the intensity of a normal γ-ray peak depends roughly on the inverse square of the distance between the source and detector, sum peaks depend on the inverse fourth power of the distance. This change of the relative intensity of the 1235.49-keV peak with distance clearly identifies it as a sum peak.

A similar situation obtains for the peak at 1710.35 keV, the intensity of which can be accounted for through the "skip-over" coincidence 416.90-(818.68)-1293.56 keV. At least 90% of the observed intensity of this peak must be due to summing, leaving only a small upper limit for a possible peak at this energy. Together, our failure to observe peaks at 458, 475, 639, and 1712 keV eliminate the need to introduce a new level at 3005 keV as originally suggested by Ardisson [39].

The calculation of the intensities of these sum peaks has been calibrated against the numerous other sum peaks that appear in the spectrum, including accidental sums (both self-coincidences such as $1097.28 + 1097.28 = 2194.56$ keV or $1293.56 + 1293.56 = 2587.12$ keV as well as "parallel" coincidences such as $1097.28 + 1507.59 = 2604.87$ keV or $416.90 + 1097.28 = 1514.18$ keV) and true sums (direct cascades such as $1097.28 + 1293.56 = 2390.84$ keV or $416.90 + 2112.29 = 2529.19$ keV as well as "skip-over" cascades such as $138.29 + 1293.56 = 1431.85$ keV).

TABLE IX. γ rays emitted in the decay of ^{116m}In.

Present work				*Nuclear Data Sheets*[a]	
E (keV)	I	E_i	E_f	E (keV)	I
99.73 *4*	0.028 *3*	2365.94	2266.16	99.81 *10*	0.020 *8*
	<0.008			116.5 *10*	0.059 *24*
124.65 *5*	0.012 *2*	2390.86	2266.16	124.75 *7*	0.012 *6*
138.29 *2*	4.36 *10*	2529.13	2390.86	138.326 *8*	3.90 *14*
163.40 *10*	0.018 *2*	2529.13	2365.94	162.6 *5*	0.083 *24*
165.72 *10*	0.016 *2*	2390.86	2225.39	165.5	0.00058
	<0.010			196.5 *5*	0.059 *24*
244.98 *5*	0.039 *3*	3046.05	2801.17	245.0 *3*	0.044 *9*
263.03 *3*	0.148 *5*	2529.13	2266.16	262.95 *8*	0.14 *3*
271.96 *4*	0.045 *4*	2801.17	2529.13	272.4 *8*	0.094 *35*
278.62 *2*	0.153 *4*	2390.86	2112.26	278.49 *8*	0.17 *2*
303.73 *4*	0.142 *7*	2529.13	2225.39	303.80 *7*	0.14 *2*
	<0.007			345.2 *8*	0.035 *12*
355.40 *2*	0.861 *10*	2112.26	1756.77	355.36 *4*	0.98 *5*
395.64 *16*	0.0080 *25*	3046.05	2650.44		
410.23 *4*	0.071 *3*	2801.17	2390.86		
416.90 *2*	32.1 *3*	2529.13	2112.26	416.86 *3*	32.8 *14*
435.18 *6*	0.027 *3*	2801.17	2365.94	434.9 *7*	0.043 *17*
	<0.004			458.5 *5*	0.083 *24*
463.21 *2*	0.855 *10*	1756.77	1293.56	463.14 *12*	0.98 *6*
	<0.010			474.9 *8*	0.020 *10*
	<0.010			500.1 *8*	0.035 *12*
517.23 *10*	0.015 *2*	3046.05	2529.13		
535.03 *5*	0.040 *3*	2801.17	2266.16	536.0 *6*	0.041 *15*
567.55 *6*	0.064 *5*	3096.80	2529.13	567.4 *9*	0.049 *15*
	<0.008			639.1 *10*	0.035 *12*
655.17 *2*	0.145 *3*	3046.05	2390.86	655.7 *4*	0.13 *5*
679.85 *8*	0.024 *4*	3046.05	2365.94	679.9 *10*	0.035 *12*
688.93 *2*	0.196 *4*	2801.17	2112.26	689.0 *3*	0.19 *3*
705.97 2	0.189 *3*	3096.80	2390.86	705.7 *3*	0.20 *3*
	<0.003			730.7 *3*	0.08 *3*
				736	<0.0035
779.92 *2*	0.291 *5*	3046.05	2266.16	780.4 *2*	0.32 *6*
	<0.005			781.1 *8*	0.130 *24*
818.68 *2*	14.3 *1*	2112.26	1293.56	818.7 *2*	13.6 *5*
830.68 *10*	0.034 *6*	3096.80	2266.16	830.9 *4*	0.062 *12*
931.83 *4*	0.106 *5*	2225.39	1293.56	932.2 *3*	0.090 *19*
972.60 *2*	0.585 *6*	2266.16	1293.56	972.4 *2*	0.538 *19*
1072.50 *20*	0.019 *6*	2365.94	1293.56	1072.3 *7*	0.024 *18*
1097.28 *2*	69.0 *7*	2390.86	1293.56	1097.3 *2*	66.6 *13*
1235.49 *3*	0.006 *3*	2529.13	1293.56	1235.5 *10*	0.11 *2*
	<0.010			1254.1 *10*	0.047 *23*
1293.56 *2*	100 *1*	1293.56	0.0	1293.54 *15*	100 *2*
1356.36 *23*	0.0093 *13*	2650.44	1293.56		
1507.59 *2*	11.7 *1*	2801.17	1293.56	1507.4 *2*	11.8 *4*
	<0.008			1536.3 *9*	0.047 *35*
1710.53 *3*	<0.010			1712.3 *10*	
1752.50 *2*	2.78 *3*	3046.05	1293.56	1753.8 *6*	2.91 *9*
1803.43 *23*	0.0105 *20*	3096.80	1293.56		
2112.29 *2*	17.8 *2*	2112.26	0.0	2112.1 *14*	18.4 *5*
2225.39 *3*	0.055 *2*	2225.39	0.0	2225.5 *8*	0.061 *10*
2265.69 *21*	0.0036 *6*	2266.16	0.0		

[a]From Ref. [37], based on data of Rabenstein [38] and Ardisson [39].

TABLE X. Energy levels in ^{116}Sn populated in the decay of ^{116m}In.

Present work		*Nuclear Data Sheets*[a]		
Level energy (keV)	β feeding (%)	Level energy (keV)	β feeding (%)	J^π
0.00		0.00		0^+
1293.56 *1*		1293.560 *8*		2^+
1756.77 *3*		1756.864 *24*		0^+
2112.26 *2*		2112.323 *15*		2^+
2225.39 *2*		2225.379 *17*		2^+
2266.16 *3*		2266.159 *19*		3^-
2365.94 *3*		2365.975 *21*		5^-
2390.86 *2*	54.2 *6*	2390.879 *18*	52.1 *12*	4^+
2529.13 *2*	32.5 *3*	2529.202 *18*	33.8 *15*	4^+
2649.92 *23*		2650.438 *23*		2^+
2801.17 *2*	10.3 *1*	2801.28 *4*	10.2 *4*	4^+
3046.05 *2*	2.82 *4*	3046.40 *9*	2.71 *10*	4^+
3096.80 *3*	0.24 *3*	3096.93 *13*	0.33 *4*	4^+

[a]From Ref. [37].

V. CONCLUSIONS

From measurements of the intensity of the γ radiations following the decays of ground and isomeric states in the odd-mass radioactive isotopes of ^{113,117,123,125}Sn, we have deduced a self-consistent set of thermal cross sections and resonance integrals for ^{112,116,122,124}Sn. For captures leading to $11/2^-$ states (^{117m,123g,125g}Sn), for which five units of angular momentum must be added to the $1/2^+$ capture state, the measured thermal cross sections are small and in quite good agreement with one another at 3–4 mb. Captures leading to other Sn isotopes with $11/2^-$ states include ^{119m}Sn (10 ± 6 mb [2]) and ^{121m}Sn (1 mb [2,8]), consistent with the systematic behavior of captures leading to the $11/2^-$ states observed in the present work.

There is also reasonable agreement among the thermal cross sections leading to the $1/2^+$ and $3/2^+$ states in the odd-mass isotopes. We have determined precise values for the $1/2^+$ state in ^{113g}Sn (for the first time clearly separating direct and indirect production) and the $3/2^+$ states in ^{123m,125m}Sn. These values are consistent with other previously measured Sn cross sections [2], including neutron captures leading to the $1/2^+$ states in ^{115g}Sn (0.12 ± 0.03 b), ^{117g}Sn (0.14 ± 0.03 b), and ^{119g}Sn (0.22 ± 0.05 b) and the $3/2^+$ state in ^{121g}Sn (0.14 ± 0.03 b). These cross sections leading to the $s_{1/2}$ and $d_{3/2}$ single-particle states are generally in the range of 0.1–0.2 b, suggesting that the states can be reached with more or less equivalent ease from the $1/2^+$ capture state. These systematic behaviors for both the $h_{11/2}$ states and the $s_{1/2}$ and $d_{3/2}$ states are a consequence of the closed proton shell in Sn, which restricts the contributions of the protons to the nuclear structure despite the addition of 12 neutrons from ^{113}Sn to ^{125}Sn. Such systematic behavior seems not to be demonstrated in neutron capture in the corresponding Te isotones, only two protons removed from Sn [42].

ACKNOWLEDGMENTS

We are grateful for the support of the Oregon State University Radiation Center and the assistance of the staff of the Oregon State TRIGA reactor in enabling these experiments to be carried out.

[1] S. F. Mughabghab, M. Divadeenam, and N. E. Holden, *Neutron Cross Sections* (Academic, New York, 1981), Vol. 1.
[2] For more recent results and a summary of recommended values, see the compilation of the National Nuclear Data Center: http://www.nndc.bnl.gov/nudat2/index.jsp.
[3] E. Browne and R. B. Firestone, *Table of Radioactive Isotopes* (Wiley, New York, 1986).
[4] http://ne.oregonstate.edu/facilities/radiation_center/ostr.html
[5] C. L. Duncan and K. S. Krane, Phys. Rev. C **71**, 054322 (2005).
[6] ORTEC, Inc. - http://www.ortec-online.com/pdf/a65.pdf.
[7] P. A. Aarnio, J. T. Routti, and J. V. Sandberg, J. Radioanal. Nucl. Chem. **124**, 457 (1988).
[8] L. Seren, H. N. Friedlander, and S. H. Turkel, Phys. Rev. **72**, 888 (1947).
[9] C. M. Nelson, B. H. Ketelle, and G. E. Boyd, Oak Ridge National Laboratory Report ORNL-828, 1950 (unpublished); results quoted in Ref. [2].
[10] M. Schmorak, G. T. Emery, and G. Scharff-Goldhaber, Phys. Rev. **124**, 1186 (1961).
[11] S. K. Mangal and P. S. Gill, Nucl. Phys. **41**, 372 (1963).
[12] W. Lyon and H. Ross, Oak Ridge National Laboratory Report ORNL-4196, 1966 (unpublished); results quoted in Ref. [2].
[13] R. S. Tilbury and H. H. Kramer, Nucl. Sci. Eng. **31**, 545 (1968).
[14] W. Maenhaut, F. Adams, and J. Hoste, J. Radioanal. Chem. **16**, 39 (1973).
[15] M. Ricabarra, R. Turjanski, and G. Ricabarra, Report INDC(ARG)-8, 1973 (unpublished); results quoted in Ref. [2].
[16] G. Gleason, Radiochem. Radioanal. Lett. **26**, 39 (1976); A corrected value of the resonance integral was communicated to the NNDC compilers and is quoted in Ref. [2].
[17] R. E. Heft, in *Proceedings of the Conference on Computers in Activation Analysis*, edited by R. Farmakes (American Nuclear Society, La Grange Park, IL, 1978).
[18] P. Nikolow and S. Niese, Isotopenpraxis **1**, 31 (1980).
[19] F. De Corte, I. Moens, A. Simonits, and J. Hoste, J. Radioanal. Nucl. Chem. **92**, 183 (1985).
[20] K. Knopf, W. Waschkowski, A. Aleksejevs, S. Barkanova, and J. Tambergs, Z. Naturforsch. A **52**, 270 (1997).
[21] S. Nakamura, K. Furutaka, H. Harada, and T. Katoh, Japan Atomic Energy Research Institute Report JAERI-Conf-99-002, 1999 (unpublished).
[22] Yu. P. Gangrsky, P. Zuzaan, N. N. Kolesnikov, V. G. Lukashik, and A. P. Tonchev, Bull. Russ. Acad. Sci. Phys. **65**, 121 (2001).
[23] L. Sage and A. K. Furr, J. Am. Nucl. Soc. **23**, 501 (1976).

[24] V. A. Anufriev, S. I. Babich, S. M. Masyanov, and V. N. Nefedov, At. Energ. **63**, 397 (1987) [Sov. J. At. Energy **63**, 912 (1987)].
[25] R. Van der Linden, F. De Corte, P. Van den Winkel, and J. Hoste, J. Radioanal. Chem. **11**, 133 (1972).
[26] F. De Corte, L. Moens, A. Simonits, A. de Wispelaere, and J. Hoste, J. Radioanal. Chem. **79**, 255 (1983).
[27] A. Simonits, F. De Corte, T. El Nimr, L. Moens, and J. Hoste, J. Radioanal. Nucl. Chem. **81**, 397 (1984).
[28] J. Blachot, Nucl. Data Sheets **83**, 647 (1998).
[29] A. Mukherjee, S. Bhattacharya, and B. Dasmahapatra, Int. J. Appl. Radiat. Isotop. **44**, 731 (1993).
[30] S. Ohya, Nucl. Data Sheets **102**, 547 (2004).
[31] S. Raman, R. L. Auble, and F. F. Dyer, Phys. Rev. C **9**, 426 (1974).
[32] V. K. Tikku, H. Singh, and S. K. Mukherjee, Nuovo Cimento A **41**, 14 (1977).
[33] J. Katakura, Nucl. Data Sheets **86**, 955 (1999).
[34] P. A. Baedecker and W. B. Walters, Nucl. Phys. **A107**, 449 (1968).
[35] G. Berzins and R. L. Auble, Nucl. Phys. **A109**, 316 (1968).
[36] Y. Kawase, K. Okano, S. Uehara, and T. Hayashi, Nucl. Phys. **A163**, 534 (1971).
[37] J. Blachot, Nucl. Data Sheets **92**, 455 (2001).
[38] D. Rabenstein, Z. Phys. **240**, 244 (1970).
[39] G. Ardisson, Radiochem. Radioanal. Lett. **16**, 241 (1974).
[40] G. Wurdiyanto, H. Miyahara, A. Yoshida, K. Yanagida, and C. Mori, J. Nucl. Sci. Technol. **32**, 1090 (1995).
[41] J. Kantele, R. Julin, M. Luontama, A. Passoja, T. Poikolainen, A. Backlin, and N.-G. Jonsson, Z. Phys. A **289**, 157 (1979).
[42] I. Tomandl, J. Honzatko, T. von Egidy, H.-F. Wirth, T. Belgya, M. Lakatos, L. Szentmiklosi, Zs. Revay, G. L. Molnar, R. B. Firestone, and V. Bondarenko, Phys. Rev. C **68**, 067602 (2003).